4 Atmospheric Dynamics and Stability

As mentioned in Chapter 1, convective clouds such as cumulus and cumulonimbus develop in unstable air due to the buoyancy force. Buoyancy is a positive, upward force experienced by objects within a fluid in a gravitational field that are less dense than their environment. In the context of cloud formation, buoyancy mainly refers to air parcels (Section 3.2) that are warmer and/or more moist than the surrounding environmental air. In atmospheric sciences, downward motions toward the ground are equally important and are experienced by air parcels that are denser than the environment.

In this chapter, we start by describing the basic equations of the reference state, from which the concept of buoyancy can be derived. Thereafter, we discuss the meaning of stability and instability in the atmosphere in the vertical, horizontal, or slantwise (at an angle between the horizontal and vertical) directions.

4.1 Navier–Stokes Equation

By expressing conservation of momentum, the general *Navier–Stokes*[1] *equation*, or *equation of motion*, is the basic equation to describe fluid motions in three dimensions (e.g., Dutton, 1976; Gill, 1982; Zdunkowski and Bott, 2003). Depending on the application, we are often only interested in either the vertical or the horizontal motion of air parcels, for example, the size of a party balloon, with uniform T and q_v, or air masses (a larger body of air with distinct boundaries and having nearly uniform T and q_v at a given altitude). Typical examples of air masses include the warm air mass behind a warm front and the cold air mass behind the cold front in low-pressure systems.

In the atmospheric sciences, we typically use forces per unit mass $\mathrm{N\,kg^{-1}} = \mathrm{m\,s^{-2}}$, which is consistent with the use of specific thermodynamic quantities as introduced in Chapter 3. In its three-dimensional form, per unit mass, the Navier–Stokes equation is given as

$$\begin{aligned} \frac{d\vec{v}}{dt} &= \vec{F}_{PG} + \vec{F}_C + \vec{F}_g + \vec{F}_F. \\ &= -\frac{1}{\rho_a}\nabla p - f\vec{k} \times \vec{v} - g\vec{k} + \vec{F}_F. \end{aligned} \tag{4.1}$$

[1] www.britannica.com/biography/Sir-George-Gabriel-Stokes-1st-Baronet

https://doi.org/10.1017/9781009485654.005 Published online by Cambridge University Press

Here, $\vec{v}$ is the three-dimensional velocity vector $\vec{v} = u\vec{i} + v\vec{j} + w\vec{k}$, where $\vec{i}, \vec{j}, \vec{k}$ denote the unit vectors in the x-, y-, and z-directions, and t is time. Thus, velocity encompasses both direction and speed. Using this notation, the x-direction is defined from west to east, the y-direction from south to north, and the z-axis points upward (perpendicular to the surface). In eq. (4.1), d/dt denotes the total time derivative:

$$\frac{d}{dt} = \frac{\partial}{\partial t} + \vec{v} \cdot \nabla, \tag{4.2}$$

where the first term denotes the local time derivative and the second term denotes the three-dimensional advection. The advection term expresses the fact that for a variable of the fluid element, in this case velocity, its changes are a result of the displacement of the fluid element along the three axes (x, y, z). The total time derivative is the same as the Lagrangian[2] time derivative and represents the total change in a quantity as seen by an observer moving with the particular fluid element.

The first term on the right-hand side of eq. (4.1) is the pressure gradient force $\vec{F}_{PG}$:

$$\vec{F}_{PG} = -\frac{1}{\rho_a} \nabla p. \tag{4.3}$$

$\vec{F}_{PG}$ represents the force acting on a fluid element along the pressure gradient ∇p and depends inversely on the air density ρ_a.

The second term on the right-hand side of eq. (4.1, $-f\vec{k} \times \vec{v}$) is the *Coriolis force*, described in the next paragraph. Given that it is a force per unit mass, it is also referred to as the Coriolis term $\vec{F}_C$. Here, $f = 2\Omega \sin\phi$ is the Coriolis parameter, where ϕ is the latitude in units of ° of the location at which the Coriolis force is calculated and $\Omega = 7.29 \times 10^{-5}\ \mathrm{s}^{-1}$ is the magnitude of the angular velocity of the Earth's rotation. In midlatitudes, f is on the order of $10^{-4}\ \mathrm{s}^{-1}$.

The third term on the right-hand side of eq. (4.1, $-g\vec{k}$) is the force arising from the acceleration due to gravity $\vec{F}_g$, which acts downward. The fourth term of eq. (4.1, $\vec{F}_F$) is the friction force, which is dominated by small-scale turbulent fluctuations. $\vec{F}_F$ also includes the terms related to the compressibility of air. These are responsible for sound waves and can be neglected on larger scales.

The Coriolis force $\vec{F}_C$ on an object results from the rotation of the Earth and is given as:

$$\vec{F}_C = -2\vec{\Omega} \times \vec{v}. \tag{4.4}$$

The Coriolis force is perpendicular both to the axis of Earth's rotation and to the object's relative velocity (i.e., the object's velocity without the contribution from Earth's rotation). Because the Coriolis force is perpendicular to the relative velocity, it does no work and hence is an "apparent" force, felt only in a rotating frame. As the axis of Earth's rotation goes from south to north, the three components of $\vec{\Omega}$ are given as:

$$\Omega_x = 0, \qquad \Omega_y = \Omega \cos\phi, \qquad \Omega_z = \Omega \sin\phi. \tag{4.5}$$

[2] www.britannica.com/biography/Joseph-Louis-Lagrange-comte-de-lEmpire

https://doi.org/10.1017/9781009485654.005 Published online by Cambridge University Press

Thus, the three components of the Coriolis force of eq. (4.4) are given as:

$$\vec{F}_C = -2 \begin{pmatrix} \Omega \cos\phi w - \Omega \sin\phi v \\ \Omega \sin\phi u \\ -\Omega \cos\phi u \end{pmatrix}. \tag{4.6}$$

Because w is much smaller than v for large-scale motions, for which the Coriolis force matters, the first term in the x-component of the Coriolis force is typically neglected. Then, the two horizontal components of the Coriolis force can be written as

$$\begin{aligned} F_{C,x} &= 2\Omega \sin\phi v = fv, \\ F_{C,y} &= -2\Omega \sin\phi u = -fu. \end{aligned} \tag{4.7}$$

The Coriolis force causes a moving air parcel in the northern hemisphere to be deflected to the right, and in the southern hemisphere to the left, from the air parcel's original direction of motion. Taking the expression of the Coriolis force and inserting it into eq. (4.1) results in the Navier–Stokes equations for the three velocity components:

$$\frac{du}{dt} = -\frac{1}{\rho_a}\frac{\partial p}{\partial x} + fv + F_{F,x}, \tag{4.8}$$

$$\frac{dv}{dt} = -\frac{1}{\rho_a}\frac{\partial p}{\partial y} - fu + F_{F,y}, \tag{4.9}$$

$$\frac{dw}{dt} = -\frac{1}{\rho_a}\frac{\partial p}{\partial z} + 2\Omega \cos\phi u - g + F_{F,z}. \tag{4.10}$$

In a rotating frame, there is another apparent force, the centripetal force. It is a reaction to the centrifugal force $\vec{F}_{CF}$ generated by the rotation. In the case of a ball on a string swung in a loop, the centripetal force is provided by the tension along the string and balances the centrifugal force exactly, so that the ball stays in orbit and does not fly off. In the case of a satellite orbiting the Earth, the centripetal force is exerted by gravity and balances the radially outward-directed pull generated by the centrifugal force.

In the Earth's rotating frame, the centrifugal force on an object is not balanced by a reactionary centripetal force, because there is no string. As the centrifugal force is small compared with other forces exerted on an object in Earth's atmosphere (e.g., gravity or the Coriolis force), it is often neglected and does not appear in the Navier–Stokes equation.

The Navier–Stokes equation (eq. 4.1) cannot be solved analytically (e.g., Dutton, 1976). It can either be solved numerically, as done in numerical weather forecast models or climate models, or it needs to be simplified. Nonetheless, by using mathematical methods such as scale analysis, it is possible to derive approximate solutions that allow us to gain insights on the major forces acting during fluid motion and thus to elucidate features of atmospheric motions. In the following sections, we will perform scale analysis of the different (x, y, z) components of the Navier–Stokes equation.

https://doi.org/10.1017/9781009485654.005 Published online by Cambridge University Press

4.2 Vertical Air Motions

4.2.1 Hydrostatic Equation

Cloud formation takes place by vertical air motions, that is, processes describing ascent and descent of air parcels and air masses. To describe such processes, we analyze the z-component of the Navier–Stokes equation, as given in eq. (4.10). To simplify this equation, we perform a scale analysis, that is, we assess the magnitudes and hence relative importance of the individual terms. Characteristic values for the individual parameters are listed in Table 4.1. By using the typical values from Table 4.1 for *synoptic* (large-scale) conditions within eq. (4.10), it can be seen that both the gravitational force ($g = 9.81\,\mathrm{m\,s^{-2}}$) and the pressure gradient force ($p_0/(\rho_a H) \sim 10\,\mathrm{m\,s^{-2}}$) are orders of magnitude larger than the Coriolis force ($fU \propto 10^{-3}\,\mathrm{m\,s^{-2}}$), which can thus be neglected. We can further simplify the z-component of the Navier–Stokes equation by neglecting the frictional force $F_{F,z}$, which is a justified assumption outside the PBL. Doing so, the z-component of the Navier–Stokes equation (eq. 4.10) can be simplified to

$$\frac{dw}{dt} = -\frac{1}{\rho_a}\frac{\partial p}{\partial z} - g. \tag{4.11}$$

To a very good approximation, the atmosphere is in hydrostatic balance, that is, the vertical acceleration dw/dt for large-scale motions is negligible. Again, this can be verified by using characteristic synoptical values from Table 4.1, yielding $dw/dt = W/t_{vert} \sim 10^{-8}\,\mathrm{m\,s^{-2}}$. When neglecting the vertical acceleration, we have a balance between the vertical pressure gradient force and the acceleration due to gravity:

Table 4.1 Scale analysis for the large-scale flow and for a small cumulus humilis (Cu hum) and a cumulonimbus cloud (Cb) (see also Table 1.3). Capital letters mark the respective characteristic scales, $_{hor}$ denotes horizontal scales and $_{vert}$ vertical scales. Note that these values differ from the values provided in Chapter 1 because here we use only order-of-magnitude estimates.

Scale	Variable	Large-scale	Cu hum	Cb
Length	$\Delta x = L$	$\sim 10^6\,\mathrm{m}$	$\sim 10^3\,\mathrm{m}$	$\sim 10^4\,\mathrm{m}$
Length	$\Delta z = H$	$\sim 10^4\,\mathrm{m}$	$\sim 10^3\,\mathrm{m}$	$\sim 10^4\,\mathrm{m}$
Velocity	$u, v, \Delta u, \Delta v = U$	$\sim 10\,\mathrm{m\,s^{-1}}$	$\sim 1\,\mathrm{m\,s^{-1}}$	$\sim 10\,\mathrm{m\,s^{-1}}$
Velocity	$w = W$	$\sim 10^{-2}\,\mathrm{m\,s^{-1}}$	$\sim 1\,\mathrm{m\,s^{-1}}$	$\sim 10\,\mathrm{m\,s^{-1}}$
Time	$\Delta t = t_{hor} = L/U$	$\sim 10^5\,\mathrm{s}$	$\sim 10^3\,\mathrm{s}$	$\sim 10^3\,\mathrm{s}$
Time	$\Delta t = t_{vert} = H/W$	$\sim 10^6\,\mathrm{s}$	$\sim 10^3\,\mathrm{s}$	$\sim 10^3\,\mathrm{s}$
Density	ρ_a	$\sim 1\,\mathrm{kg\,m^{-3}}$	$\sim 1\,\mathrm{kg\,m^{-3}}$	$\sim 1\,\mathrm{kg\,m^{-3}}$
Acceleration	$\Delta u/\Delta t = U/t_{hor}$	$\sim 10^{-4}\,\mathrm{m\,s^{-2}}$	$\sim 10^{-3}\,\mathrm{m\,s^{-2}}$	$\sim 10^{-2}\,\mathrm{m\,s^{-2}}$
Acceleration	$\Delta w/\Delta t = W/t_{vert}$	$\sim 10^{-8}\,\mathrm{m\,s^{-2}}$	$\sim 10^{-3}\,\mathrm{m\,s^{-2}}$	$\sim 10^{-2}\,\mathrm{m\,s^{-2}}$
Pressure	Δp_{hor}	$\sim 10^3\,\mathrm{Pa}$	$\sim 10\,\mathrm{Pa}$	$\sim 10\,\mathrm{Pa}$

https://doi.org/10.1017/9781009485654.005 Published online by Cambridge University Press

$$\frac{\partial p}{\partial z} = -g\rho_a. \tag{4.12}$$

Equation (4.12) is called the *hydrostatic equation*. We point out that for cloud formation or in-cloud processes, the assumption of hydrostatic equilibrium is most often not valid, because vertical acceleration cannot be neglected anymore. This cannot be seen by performing a scale analysis for the z-component of the Navier–Stokes equation using the characteristic values for Cu hum or for Cb given in Table 4.1. An analysis based on these values would reveal that the vertical acceleration for Cu hum of $dw/dt = W/t_{vert} \sim 10^{-3}\,\mathrm{m\,s^{-2}}$ or Cb of $dw/dt = W/t_{vert} \sim 10^{-2}\,\mathrm{m\,s^{-2}}$ is still orders of magnitude smaller than the vertical pressure gradient force or acceleration due to gravity. Instead, when studying processes in convective clouds, deviations from the surrounding air will be studied, because locally acceleration is very important (Section 4.2.3).

4.2.2 Hypsometric Equation

As a result of the variable moisture content of environmental air, it is common in atmospheric science to express the air density ρ_a in terms of p and the virtual temperature T_v (eq. 3.97) using the ideal gas law (eq. 3.94). Doing this in eq. (4.12), we obtain

$$\frac{\partial p}{\partial z} = -g\frac{p}{R_d T_v}, \tag{4.13}$$

where R_d is the gas constant of dry air (eq. 3.8). To replace the partial derivative with the total derivative, we need to assume that T_v is not a function of p. If we restrict the integration of eq. (4.13) to a sufficiently small z-interval, we can replace T_v by its average value $\overline{T_v}$ over that z-interval. Therefore, after rearranging terms, we get

$$\frac{dp}{p} = -\frac{g}{R_d \overline{T_v}}\,dz. \tag{4.14}$$

Integration of this equation between z_0 and z on the right-hand side and the corresponding pressure interval between p_0 and p on the left-hand side yields the hypsometric equation:

$$p = p_0 \exp\left[-\frac{g}{R_d \overline{T_v}}(z - z_0)\right]. \tag{4.15}$$

Using the hypsometric equation, the pressure p at an altitude z can be calculated from $\overline{T_v}(z)$ together with knowledge of the pressure p_0 at a starting altitude z_0.

4.2.3 Buoyancy Force

An air parcel will undergo vertical displacements from the environmental air if a buoyancy force F_B acts on it. The buoyancy force acting on an air parcel is caused by the difference in density between an air parcel and the surrounding atmosphere. A displacement of an air parcel results from a perturbation of the reference state of the environmental air, which we assume to

https://doi.org/10.1017/9781009485654.005 Published online by Cambridge University Press

be in hydrostatic equilibrium, called *hydrostatic balance*. Furthermore, we assume that the air parcel is always at the same pressure as the environmental air at any given altitude.

The starting point to derive an expression for the buoyancy force is the vertical component of the Navier–Stokes equation (eq. 4.1). However, this time we use it in its perturbation form, which means that we are interested in deviations from the mean quantities. This is done by employing Reynolds decomposition[3], which means that the perturbations are defined such that their time average equals zero. In the case of the vertical velocity, we denote the mean vertical velocity by $\overline{w}$ and the deviation from the mean, that is, the perturbation, by $\tilde{w}$:

$$w = \overline{w} + \tilde{w}. \tag{4.16}$$

Neglecting friction ($F_{F,z}$) and the Coriolis force ($F_{C,z}$), the vertical component (eq. 4.11) of the Navier–Stokes equation is

$$\frac{d}{dt}(\overline{w} + \tilde{w}) = -\frac{1}{(\overline{\rho_a} + \tilde{\rho_a})}\frac{\partial(\overline{p} + \tilde{p})}{\partial z} - g. \tag{4.17}$$

Here, we made use of $p = \overline{p} + \tilde{p}$ and $\rho_a = \overline{\rho_a} + \tilde{\rho_a}$, in analogy to eq. (4.16). The large-scale environment, that is, the mean state of the environmental air, is assumed to be in hydrostatic balance ($\frac{d\overline{w}}{dt} = 0$). Using the hydrostatic balance eq. (4.12) to replace g, eq. (4.17) becomes

$$\begin{aligned}
\frac{d\tilde{w}}{dt} &= -\frac{1}{(\overline{\rho_a} + \tilde{\rho_a})}\frac{\partial(\overline{p} + \tilde{p})}{\partial z} + \frac{1}{\overline{\rho_a}}\frac{\partial \overline{p}}{\partial z} \\
&= \frac{\tilde{\rho_a}}{(\overline{\rho_a} + \tilde{\rho_a})\overline{\rho_a}}\frac{\partial \overline{p}}{\partial z} - \frac{1}{(\overline{\rho_a} + \tilde{\rho_a})}\frac{\partial \tilde{p}}{\partial z} \\
&= -\frac{\tilde{\rho_a}}{\rho_a}g - \frac{1}{\rho_a}\frac{\partial \tilde{p}}{\partial z} \\
&= -\left(\frac{\rho_a - \overline{\rho_a}}{\rho_a}\right)g - \frac{1}{\rho_a}\frac{\partial \tilde{p}}{\partial z}.
\end{aligned} \tag{4.18}$$

We now associate the quantities of the environmental atmosphere (index "*env*") with the mean state (e.g., $\overline{\rho_a}$), and the parcel's properties with the actual state (e.g., ρ_a). In eq. (4.18), the first term on the right-hand side is the acceleration that arises due to buoyancy. This acceleration is referred to as the buoyancy force F_B and is given as

$$F_B = g\left(\frac{\rho_{a,env} - \rho_a}{\rho_a}\right). \tag{4.19}$$

Differences in density between the air parcel ρ_a and the environmental air $\rho_{a,env}$ give rise to buoyancy. The buoyant force is positive, that is, it is directed upwards, when the parcel is less dense than the environmental air. Density fluctuations occur due to perturbation in temperature, pressure, water vapor, or condensed water. For cloud formation, the temperature perturbations are usually the dominant factor for density perturbations. Exceptions are severe convective storms (Chapter 11), for which pressure perturbations can be equally important and where water loading and latent heat consumption can cause severe downdrafts. Considering only temperature perturbations, eq. (4.19) can be approximated as:

[3] https://glossarytest.ametsoc.net/wiki/Reynolds_averaging

https://doi.org/10.1017/9781009485654.005 Published online by Cambridge University Press

$$F_B \approx g\left(\frac{T_v - T_{v,env}}{T_{v,env}}\right), \tag{4.20}$$

where $T_{v,env}$ is the environmental virtual temperature. This simplified, temperature-based buoyancy equation will be used throughout this chapter. Limitations of this assumption will be discussed in Section 5.2.6. As a further simplification and to be able to also use eq. (4.20) for estimating buoyancy for moist air processes in a tephigram, where T_v cannot be inferred, we refrain from differentiating between T and T_v when using a tephigram to analyze air parcel buoyancy, as well as for the stability analysis in Sections 4.3 and 4.4.

4.3 Static Stability in Water-subsaturated Air

As we saw in Chapter 3, as long as an air parcel ascends prior to the onset of condensation in moist air, that is, as long as the air parcel is subsaturated with respect to liquid water, the ascent of the air parcel follows the dry adiabat. Beyond condensation, the air parcel follows the saturated or moist adiabat. The temperature changes differently with altitude along the dry and saturated adiabats, which has implications for the stability of the atmosphere. Therefore, it is important to distinguish between stability in water-subsaturated air, which denotes the absence of hydrometeors, and in condensing air, which contains hydrometeors.

The question of stability or instability refers to the reaction of a system to perturbations. A system is in a situation of stable equilibrium if, after a perturbation (a displacement, an impulse, etc.), a restoring force brings the system back to the initial state. The onset of a perturbation in a state of unstable equilibrium, on the contrary, leads to further deviation from the initial conditions. A ball on the tip of a mountain is an example of the latter state, as a small displacement will cause it to fall or roll down the mountain. In the atmosphere, perturbations causing instabilities are, for example, local heating or cooling of the air flowing over a mountain ridge. Air flowing over mountainous regions can initiate perturbations in the form of stationary lee waves, illustrated in Figure 4.1. The downwind oscillary motion associated with these lee waves can lead to cloud formation. Because the flow describes a damped oscillatory motion with several ascents and descents, seemingly stationary clouds can form wherever the air ascends and the LCL is reached. In Figure 4.1, a cirrus cloud with varying thicknesses depending on the phase of the wave, and two Ac len clouds (Figure 1.11f) are shown. The wavelengths and amplitudes of these stationary lee waves are typically on the order of 5–10 km and 100–200 m, respectively, depending on the geometry of the mountain ridge (Richner and Hächler, 2013). Just above the mountain crest in Figure 4.1, a Foehn wall cloud (Figure 3.18) is depicted. Behind the cloud-free Foehn gap, a rotor cloud with a cumulus fractus below it is visible in the horizontally rotating air mass. Such rotors are often associated with severe turbulence.

In the mountain lee, the sinking and warming air masses are transported over colder air in the cold pool. Mixing of the cold air with the warmer overlying air can cause mixing fog (Figure 1.12) by the same mechanism by which fog appears over a cold lake when warm air

https://doi.org/10.1017/9781009485654.005 Published online by Cambridge University Press

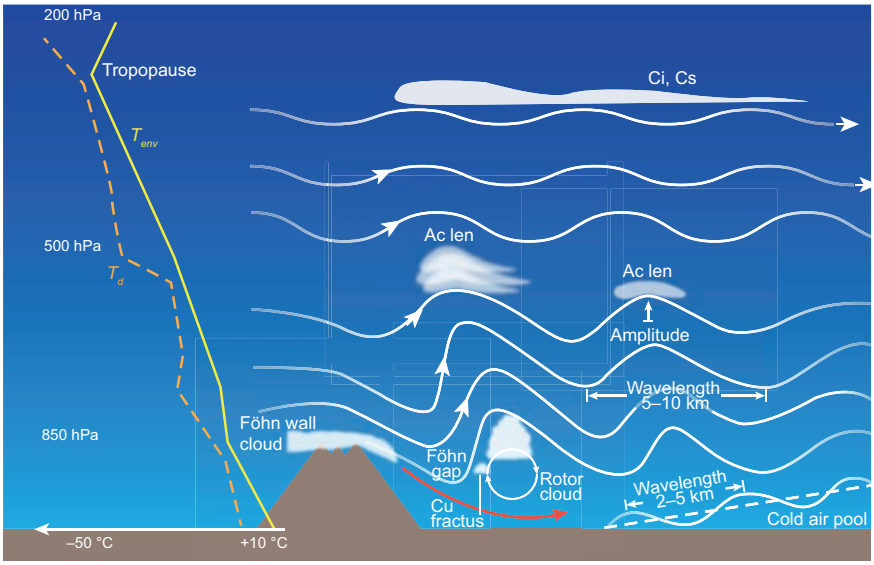


Figure 4.1 Schematic of different cloud types formed as a result of oscillatory motions initiated by an air mass flowing over a mountain ridge, along with an illustration of vertical profiles of the environmental air temperature and the dew point temperature, respectively. Wavelengths are taken from Richner and Hächler (2013).

blows over it (Section 5.1). The temperature and the resulting density differences between the warm and cold air masses cause gravity waves with wavelengths of 2–5 km (Nappo, 2012) to develop on top of the cold pool (Figure 4.1).

In the atmosphere, hydrostatic (often abbreviated to "static") stability depends on the density of the air parcel compared to the density of the environmental air, that is, on whether the temperature/moisture of an air parcel is lower or higher than the surrounding air. According to eq. (4.20), a warmer and/or moister air parcel leads to a buoyancy force and the air parcel rises. On the contrary, for a colder and/or drier air parcel, gravity dominates and the air parcel sinks.

The vertical stability therefore depends on the vertical temperature and moisture distribution in the atmosphere, which can be measured by a *radiosonde* on a weather balloon. During the ascent of the radiosonde that is equipped with a global positioning system sensor to determine height, wind speed, and wind direction, and instruments for measuring T and q_v. The data is transmitted to the measurement station at the ground. The data of these radiosondes are usually depicted in thermodynamic charts, for example, in a tephigram, and provide key information for climate research and weather prediction. Global radiosonde data can be obtained from the University of Wyoming[4] and from the GRUAN network[5]. In Switzerland, the Federal Office of Meteorology and Climatology, MeteoSwiss, conducts two radiosonde measurements per day from their measurement site in Payerne[6], which we make use of in Chapters 5 and 11.

[4] https://weather.uwyo.edu/upperair/bufrraob.shtml
[5] www.gruan.org/
[6] www.meteoschweiz.admin.ch/service-und-publikationen/applikationen/radiosondierungen.html

https://doi.org/10.1017/9781009485654.005 Published online by Cambridge University Press

Figure 4.1 depicts an illustration of such a radiosonde measurement, showing vertical profiles of T_{env} and T_d, which together with the oscillatory air motions, cause the formation of the various clouds depicted. The change in the environmental temperature with height is called the *environmental lapse rate* $\gamma = -\partial T_{env}/\partial z$.

4.3.1 Dry Adiabatic Lapse Rate

In subsaturated air, the air parcel ascends and descends dry-adiabatically according to a dry adiabatic lapse rate Γ_d. Γ_d describes the rate at which the temperature of the parcel changes with altitude. Note that Γ is a process lapse rate that describes the motion of an air parcel, while the environmental lapse rate γ represents the change of the environmental temperature with height.

The dry adiabatic lapse rate Γ_d can be derived from the first law of thermodynamics (eq. 3.26), assuming that the air parcel undergoes adiabatic transformations, that is, $dq = 0$, and that the atmosphere is in hydrostatic equilibrium:

$$dq = 0 = -\alpha dp + c_p dT. \tag{4.21}$$

Rearranging terms and making use of the hydrostatic equation (4.12) yields

$$c_p dT = \alpha dp = \frac{1}{\rho_a} dp = -g dz. \tag{4.22}$$

Note that we have replaced the partial derivatives in the hydrostatic equation by total derivatives because there are no other dependencies. Dividing by $c_p dz$ then gives Γ_d:

$$\Gamma_d \equiv -\left(\frac{dT}{dz}\right)_{dry} = \frac{g}{c_p} \sim 9.8\,\mathrm{K\ km^{-1}}. \tag{4.23}$$

In the atmosphere, an environmental lapse rate as large as the dry adiabatic lapse rate is only found in areas where the moisture content is very small. Examples of this are within the PBL over deserts, or the upper troposphere. Condensation of water vapor reduces the environmental lapse rate due to the release of latent heat, which will be discussed in Section 4.4.

4.3.2 Dry Adiabatic Lapse Rate and Static Stability

The environmental lapse rate γ can be related to the vertical gradient of the potential temperature θ of the environmental air. To see that, we start from the partial derivative of θ with altitude using the definition of θ (Section 2.2.5 and eq. 3.42):

$$\frac{1}{\theta}\frac{\partial \theta}{\partial z} = \frac{1}{\theta}\frac{\partial}{\partial z}\left[T_{env}\left(\frac{p_0}{p}\right)^{\kappa}\right] = \frac{1}{T_{env}}\frac{\partial T_{env}}{\partial z} - \frac{\kappa}{p}\frac{\partial p}{\partial z}. \tag{4.24}$$

https://doi.org/10.1017/9781009485654.005 Published online by Cambridge University Press

Table 4.2 Static stability criteria in subsaturated air.

$\gamma < \Gamma_d \leftrightarrow \partial\theta/\partial z > 0$	Stable atmosphere
$\gamma = \Gamma_d \leftrightarrow \partial\theta/\partial z = 0$	Neutral atmosphere
$\gamma > \Gamma_d \leftrightarrow \partial\theta/\partial z < 0$	Unstable atmosphere

By replacing $\partial p/\partial z$ with $-g\rho_a$ (hydrostatic equation, eq. 4.12), inserting the definitions of the environmental lapse rate, and using $\kappa = R_d/c_p$, we obtain

$$\frac{1}{\theta}\frac{\partial\theta}{\partial z} = -\frac{\gamma}{T_{env}} + \frac{R_d}{c_p\, p} g\rho_a. \tag{4.25}$$

The last term can be simplified by making use of the definition of the parcel's lapse rate and the ideal gas law for dry air. For this analysis, we neglect the difference between T and T_v as well as between T_{env} and $T_{v,env}$. This yields the desired relationship between the vertical gradient of the potential temperature and atmospheric stability:

$$\frac{1}{\theta}\frac{\partial\theta}{\partial z} = -\frac{\gamma}{T_{env}} + \frac{\Gamma_d}{T_{env}} = \frac{1}{T_{env}}(\Gamma_d - \gamma). \tag{4.26}$$

Equation (4.26) states that an increase in the potential temperature of the environmental air with altitude ($\partial\theta/\partial z > 0$) corresponds to an environmental lapse rate γ that is smaller than the dry adiabatic lapse rate Γ_d of the air parcel. $\gamma < \Gamma_d$ denotes a statically stable atmosphere or in short, a stable atmosphere. Under these circumstances, a small displacement in the positive z-direction cools the air parcel more than the surrounding environment, leading to a negative F_B due to gravity that pushes the air parcel down to its original position. The same effect, causing a positive F_B, is produced by displacements in the negative z-direction.

If the two lapse rates are equal ($\gamma = \Gamma_d$), that is, the potential temperature does not change with altitude ($\partial\theta/\partial z = 0$), the air parcel remains in hydrostatic equilibrium after a small displacement, and no force acts upon it. This situation is called a statically neutral stratification.

In a statically unstable atmosphere ($\gamma > \Gamma_d$), lifted air parcels continue to rise. This is equivalent to $\partial\theta/\partial z < 0$ (Table 4.2). An unstable atmosphere is extremely short-lived because turbulence, and if this is not sufficient also convection (Section 5.2), mix the air vertically until it is neutral again.

4.3.3 Brunt–Väisälä Frequency

The air parcel's equation of motion can be derived if F_B is related to the static stability, that is, to the change in θ with height. Assume that the parcel is subject to a small displacement $\tilde{z}$ around the starting point z_0, that is, $\tilde{z} = z - z_0$. In this case, we can use a Taylor series expansion to obtain a linear term for the change in the parcel's temperature T with altitude z,

https://doi.org/10.1017/9781009485654.005 Published online by Cambridge University Press

$$T(z) \approx T(z_0) + \left.\frac{dT}{dz}\right|_{z=z_0} (z - z_0), \tag{4.27}$$

and likewise for the environmental temperature,

$$T_{env}(z) \approx T_{env}(z_0) + \left.\frac{dT_{env}}{dz}\right|_{z=z_0} (z - z_0). \tag{4.28}$$

Assume that the temperature of the air parcel and the environment are the same in equilibrium at z_0 ($T(z_0) = T_{env}(z_0)$), so that subtraction of eq. (4.28) from eq. (4.27) yields:

$$T(z) - T_{env}(z) \approx \left(\left.\frac{dT}{dz}\right|_{z=z_0} - \left.\frac{dT_{env}}{dz}\right|_{z=z_0} \right) (z - z_0). \tag{4.29}$$

Inserting this into the numerator of eq. (4.20) yields:

$$F_B = \frac{d^2\tilde{z}}{dt^2} \approx \frac{g}{T_{env}} \left(\left.\frac{dT}{dz}\right|_{z=z_0} - \left.\frac{dT_{env}}{dz}\right|_{z=z_0} \right) (z - z_0). \tag{4.30}$$

We further approximate T_{env} by T in the denominator, insert the expressions for the lapse rates, and note that $z - z_0 = \tilde{z}$:

$$\frac{d^2\tilde{z}}{dt^2} = \frac{g}{T} (-\Gamma_d + \gamma)\, \tilde{z}. \tag{4.31}$$

Lastly, we replace the difference in lapse rates by the vertical gradient in θ (eq. 4.26):

$$\frac{d^2\tilde{z}}{dt^2} = -\frac{g}{\theta} \left(\frac{\partial \theta}{\partial z} \right) \tilde{z}, \tag{4.32}$$

and introduce the *Brunt–Väisälä frequency* N_{BV} in s^{-1}, which is given as

$$N_{BV} = \sqrt{\frac{g}{\theta} \frac{\partial \theta}{\partial z}}. \tag{4.33}$$

Then eq. (4.32) can be associated with the equation of motion for an harmonic oscillator (e.g., Seaborn, 2002) with frequency N_{BV} in a stable atmosphere:

$$\frac{d^2\tilde{z}}{dt^2} = -N_{BV}^2 \tilde{z}. \tag{4.34}$$

The solution of eq. (4.34) is of the form $\tilde{z}(t) = A \exp(\pm i N_{BV} t)$. If $N_{BV}^2 > 0$, that is, in a statically stable atmosphere, the subsaturated air parcel performs an oscillatory motion, where the parcel moves up and down, as shown by the waves in Figure 4.1, with the buoyancy force acting as a restoring force. If $N_{BV}^2 = 0$, the atmosphere is in neutral equilibrium with no forces acting on the subsaturated parcel. For $N_{BV}^2 < 0$, that is, in unstable conditions, there is no oscillatory motion, but $\tilde{z}(t)$ increases exponentially with time until the subsaturated air parcel

https://doi.org/10.1017/9781009485654.005 Published online by Cambridge University Press

reaches stable conditions again. In the last case, the association of N_{BV}^2 with a frequency is misleading.

A typical value of N_{BV} in midlatitudes in the troposphere between 2 and 8.5 km altitude is $0.01\,s^{-1}$ (Tsuda et al., 1991), so that the period of oscillation is $2\pi/N_{BV} = 10\,min$. The oscillatory motion of an air mass in a statically stable atmosphere can be observed when Ac len clouds form behind a mountain ridge, as shown in Figure 4.1. In this case, the oscillatory motion is triggered as the air crosses a mountain ridge and the air is moist enough to reach the LCL, as illustrated by the vertical profiles of T_{env} and T_d in Figure 4.1. Note that in the case where the oscillatory motion allows the air to reach the LCL in Figure 4.1, its equation of motion is no longer governed by $\Gamma_d - \gamma$ or $(1/\theta)\partial\theta/\partial z$ but by $\Gamma_s - \gamma$ or $(1/\theta_e)\partial\theta_e/\partial z$ (Section 4.4), where Γ_s is the saturated adiabatic lapse rate, which depends on temperature and pressure. This means that no single Brunt–Väisälä frequency can be associated with an oscillatory motion in moist air.

4.4 Static Stability in Condensing Air

We have seen that for (water-) subsaturated air, that is, in the absence of condensation, the atmosphere is stable if the environmental lapse rate is smaller than the process lapse rate for a dry adiabatic air parcel ascent. We can formulate similar conditions for the stability of the atmosphere with respect to the ascent of a saturated air parcel once the air parcel is above its LCL. For this, we need to compare the environmental lapse rate with the process lapse rate Γ_s of the saturated adiabatic ascent, that is, the rate of temperature change with height of an air parcel in which all the water vapor above 100 % RH_w condenses and RH_w then remains at 100 % (Section 3.5). We start from the first law of thermodynamics, accounting for latent heat release due to condensation (eq. 3.102), assuming adiabatic conditions ($dq = 0$), and using hydrostatic balance:

$$dq = c_p dT - \alpha dp + L_v\, dq_s = c_p dT + g dz + L_v\, dq_s. \tag{4.35}$$

Now we divide both sides by $c_p dz$ and rearrange terms:

$$\frac{dT}{dz} = -\frac{L_v}{c_p}\frac{dq_s}{dz} - \frac{g}{c_p}. \tag{4.36}$$

Replacing g/c_p with Γ_d (eq. 4.23) and writing the change in q_s as a function of temperature instead of altitude yields:

$$\frac{dT}{dz} = -\frac{L_v}{c_p}\frac{dq_s}{dT}\frac{dT}{dz} - \Gamma_d. \tag{4.37}$$

Rearranging terms then yields the saturated adiabatic lapse rate Γ_s

$$\Gamma_s \equiv -\left(\frac{dT}{dz}\right)_{saturated} = \Gamma_d \left(1 + \frac{L_v}{c_p}\frac{dq_s}{dT}\right)^{-1}. \tag{4.38}$$

https://doi.org/10.1017/9781009485654.005 Published online by Cambridge University Press

Note that for the derivation of eq. (4.38), we have assumed that the water vapor in the air parcel undergoes condensation and forms liquid water upon reaching saturated conditions. If instead the air parcel was at sufficiently low temperatures where ice is the thermodynamically stable phase, the water vapor would deposit on ice crystals instead and we would need to use the latent heat of sublimation L_s instead of the latent heat of vaporization L_v. For simplicity, here we consider the case of condensation only.

An analytical expression for Γ_s can be obtained by starting from the first law of thermodynamics, considering latent heat release (eq. 3.102) and noting that in an adiabatic process, $dq = 0$:

$$0 = c_p dT + L_v dq_v - \alpha\, dp. \tag{4.39}$$

Inserting $\rho_a = 1/\alpha$ and solving eq. (4.39) at saturation ($q_v = q_s$), yields:

$$0 = c_p dT - \frac{1}{\rho_a} dp + L_v dq_s. \tag{4.40}$$

We now replace dq_s by logarithmically differentiating the approximate form of eq. (3.88):

$$\frac{dq_s}{q_s} = \frac{de_{s,w}}{e_{s,w}} - \frac{dp}{p}. \tag{4.41}$$

Upon using the hydrostatic equation (eq. 4.12), we obtain:

$$-L_v q_s \left(\frac{de_{s,w}}{e_{s,w}} - \frac{dp}{p} \right) = c_p dT + g dz. \tag{4.42}$$

Dividing by $c_p dz$ and solving for dT/dz yields:

$$-\frac{dT}{dz} = \frac{L_v}{c_p} q_s \left(\frac{1}{e_{s,w}} \frac{de_{s,w}}{dz} + \frac{g}{R_d T} \right) + \frac{g}{c_p}. \tag{4.43}$$

Using the chain rule, we can write $de_{s,w}/dz$ as:

$$\frac{de_{s,w}}{dz} = \frac{de_{s,w}}{dT} \frac{dT}{dz}. \tag{4.44}$$

Inserting this expression into eq. (4.43) and bringing both dT/dz terms to the left yields:

$$-\frac{dT}{dz} \left(1 + \frac{de_{s,w}}{dT} \frac{L_v}{c_p} \frac{q_s}{e_{s,w}} \right) = \frac{g}{c_p} \left(\frac{L_v q_s}{R_d T} + 1 \right). \tag{4.45}$$

Inserting the Clausius–Clapeyron equation (eq. 3.70), using $\Gamma_d = -g/c_p$ and $\Gamma_s = -dT/dz$, ultimately yields the approximate analytical solution of Γ_s:

$$\Gamma_s = \Gamma_d \left(\frac{1 + \frac{L_v q_s}{R_d T}}{1 + \frac{L_v^2 q_s}{c_p R_v T^2}} \right). \tag{4.46}$$

https://doi.org/10.1017/9781009485654.005 Published online by Cambridge University Press

In analogy to the subsaturated case, the atmosphere will counteract the ascent of a saturated air parcel if $\gamma < \Gamma_s$ and promote its ascent if $\gamma > \Gamma_s$. Note that in contrast to Γ_d, Γ_s is not constant but depends on T and p because q_s depends on these parameters (eq. 3.88). As dq_s/dT is always positive, because it is proportional to $de_{s,w}/dT$, which in turn is always positive according to eq. (3.70), the absolute value of Γ_s is always smaller than Γ_d. This arises because the release of latent heat continuously heats the rising air parcel in a saturated adiabatic ascent and counteracts some of the cooling due to adiabatic expansion, so that the net cooling rate is lower than in the case of a dry adiabatic ascent.

The average value of the environmental lapse rate between the surface and the tropopause is $6.5\,\mathrm{K\,km^{-1}}$ for the International Standard Atmosphere (ISA)[7]. The ISA provides average values of pressure, temperature, and air density that are representative for conditions at 40 °N (Table 4.3). For any given day, the radiosonde profiles are different from these average values. This is because longwave cooling and/or solar heating destabilize the atmosphere, requiring mixing, turbulence, and/or convection (Chapter 5) to bring the atmosphere back to neutral conditions through vertical mixing. The saturated adiabatic lapse rate Γ_s can decrease to $4\,\mathrm{K\,km^{-1}}$ near the ground in warm humid air in the tropics. Near the tropopause, Γ_s approaches Γ_d because at these low temperatures, the moisture capacity of air is very small. This is also reflected in tephigrams such as the one shown in Figure 4.2, where the saturated adiabats approach the dry adiabats at low pressure.

Having derived Γ_s for processes of a saturated air parcel, we can now combine the results with the subsaturated case and obtain more general static stability criteria, as shown in Figure 4.2 and summarized in Table 4.4. Instead of an unsaturated stable atmosphere, we now have an absolutely stable atmosphere in the case where the environmental lapse rate is smaller than that of the saturated adiabat, which automatically also means that it is smaller than that of the dry adiabat. Processes that stabilize the atmosphere are radiative cooling of the surface, advection of warm air above colder air, mixing, and convection. If, however, the environmental lapse rate exceeds that of the dry adiabat, we have absolutely unstable conditions. The term "absolutely" in this case means that the situation is unstable no matter if the air parcel ascends dry or saturated adiabatically. Processes causing an absolutely unstable atmosphere are local surface heating or cooling aloft. An absolutely unstable atmosphere is typically short-lived and the instability is eliminated by vertical mixing (Chapter 5).

We now consider the case where the environmental lapse rate lies between the dry adiabat and the saturated adiabat. In this case, the stability depends on whether the air parcel is saturated and ascends saturated adiabatically or whether it is unsaturated and ascends dry adiabatically. If the air parcel ascends dry adiabatically then the atmosphere is statically stable, but if it is a saturated adiabatic ascent, the atmosphere is unstable. This situation is called *conditionally unstable* to indicate that the stability of the atmosphere depends on the condition of the air parcel. If the atmospheric lapse rate equals that of the dry adiabat, we have the dry neutral case where no forces support or inhibit the dry adiabatic ascent of an air parcel. If the atmospheric lapse rate equals the saturated adiabat, we have the saturated neutral case.

[7] www.iso.org/standard/7472.html

https://doi.org/10.1017/9781009485654.005 Published online by Cambridge University Press

Table 4.3 Approximate pressure, air density, and temperature as a function of height based on the ISA, representative for 40 °N (www.digitaldutch.com/atmoscalc/).

z (km)	p (hPa)	ρ_a (kgm^{-3})	T (K)
0	1013.25	1.2250	288.15
1	898.75	1.1116	281.65
2	794.95	1.0065	275.15
3	701.09	0.9091	268.65
4	616.40	0.8191	262.15
5	540.20	0.7361	255.65
6	471.81	0.6597	249.15
7	410.61	0.5895	242.65
8	356.00	0.5252	236.15
9	307.43	0.4663	229.65
10	264.36	0.4127	223.15
11	226.32	0.3639	216.65
12	193.30	0.3108	216.65
13	165.10	0.2655	216.65
14	141.02	0.2268	216.65
15	120.45	0.1937	216.65
16	102.88	0.1654	216.65
17	87.87	0.1413	216.65
18	75.05	0.1207	216.65
19	64.10	0.1031	216.65
20	54.75	0.0880	216.65
21	46.78	0.0749	217.65
22	40.00	0.0637	218.65
23	34.22	0.0543	219.65
24	29.30	0.0463	220.65
25	25.11	0.0395	221.65
30	11.72	0.0180	226.65
35	5.59	0.0082	237.05
40	2.78	0.0039	251.05
45	1.43	0.0019	265.05
50	0.76	0.0010	270.65

https://doi.org/10.1017/9781009485654.005 Published online by Cambridge University Press

Table 4.4 General static stability criteria in moist and possibly condensing air.

$\gamma < \Gamma_s$	Absolutely stable
$\gamma = \Gamma_s$	Saturated neutral
$\Gamma_s < \gamma < \Gamma_d$	Conditionally unstable
$\gamma = \Gamma_d$	Dry neutral
$\gamma > \Gamma_d$	Absolutely unstable

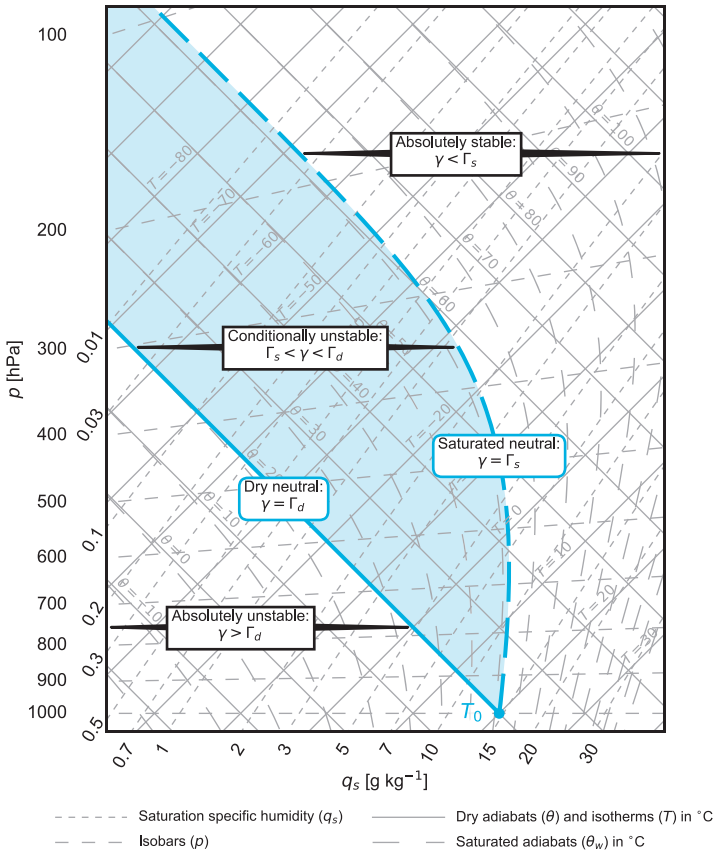


Figure 4.2 Illustration of the different kinds of vertical instabilities for an air parcel starting at T_0 and p_0 with 20 °C and 1000 hPa. The conditionally unstable area is shown in blue, and the absolutely unstable and absolutely stable areas encompass everything to the left and right, respectively, of the blue area. The dry neutral and saturated neutral conditions occur only along the dry and saturated adiabats, respectively.

https://doi.org/10.1017/9781009485654.005 Published online by Cambridge University Press

4.5 Instability of Layers

A different kind of vertical instability is *potential instability*, which is also referred to as convective instability. The stability of a layer of air can change if the entire layer is lifted. The lifting of an entire layer is likely to happen when an air mass is forced to rise over orography or when warm air is lifted above cold air at warm or cold fronts.

We start with the lifting of layers in dry air. The weight of an air column between heights z_1 and z_2 per unit area is $\int_{z_1}^{z_2} \rho_a dz$. Using the hydrostatic equation, this equals $\int_{p_2}^{p_1} (1/g)dp$. Because g is constant, we can integrate this expression to $(p_1 - p_2)/g$. In a vertical displacement, the pressure difference within the layer ($\Delta p = p_1 - p_2$) is constant due to the conservation of mass. Assuming a constant density ρ_a over the air column, we can apply the hydrostatic equation again:

$$\Delta p = -g\rho_a \Delta z, \tag{4.47}$$

where $\Delta z = z_1 - z_2$. At its base, let the potential temperature be θ_1, and at its top θ_2. After lifting, the potential temperatures at the base and top of the air column still have the values θ_1 and θ_2 since the lifting occurs dry adiabatically in a dry atmosphere. Therefore, $\Delta\theta = \theta_1 - \theta_2$ also remains constant. Since ρ_a decreases with altitude, the lifting of the layer results in a stretching of the column according to eq. (4.47). As $\Delta\theta$ can be written as $\Delta\theta = (\partial\theta/\partial z)/\Delta z =$ constant, this means that after the lifting, $|\partial\theta/\partial z|$ is smaller than before the lifting (Figure 4.3).

As an initially unstable layer (where $\partial\theta/\partial z < 0$) becomes less unstable and an initially stable layer (where $\partial\theta/\partial z > 0$) becomes less stable upon lifting, lifting shifts the lapse rate toward

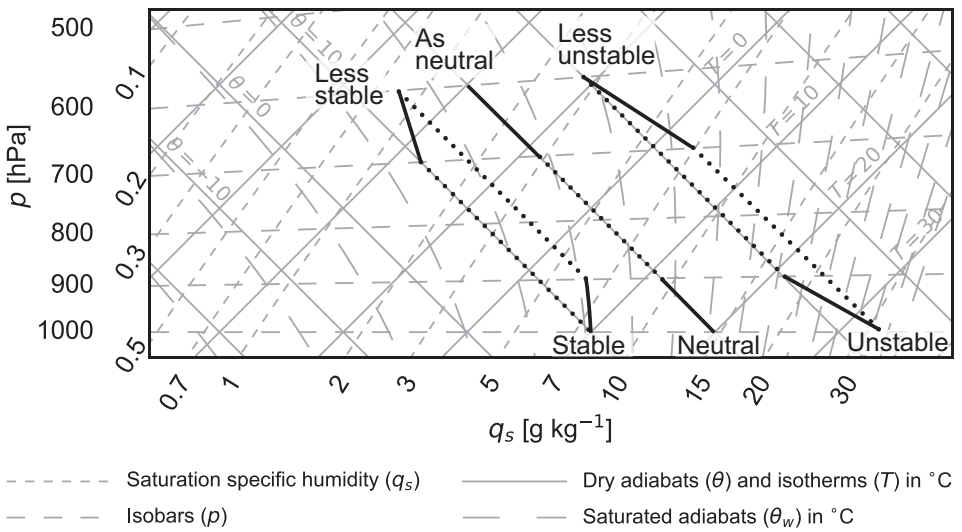


Figure 4.3 Schematic of the lifting of a layer of water-subsaturated air from 1000–900 hPa to 700–600 hPa for three cases, where the layer is initially stable, neutral, or unstable (from left to right). The bold solid lines represent the lapse rates of the layer before and after the lifting. The dotted lines show the ascent of the top and base of the layers.

https://doi.org/10.1017/9781009485654.005 Published online by Cambridge University Press

that of the dry adiabat, as illustrated in Figure 4.3. Note that although the degree of stability or instability changes upon lifting, an initially stable dry layer cannot become unstable upon lifting in a dry atmosphere nor can an initially unstable dry layer become stable upon lifting. Only the stability of neutrally stable air is unaffected by vertical displacement.

The situation becomes more complicated in moist air, where condensation can occur during the lifting process. Whether there is potential instability depends on the distribution of humidity in the atmosphere. Thus, the lifting of a layer of moist air can transform an initially stable air mass into an unstable or conditionally unstable state. The presence of a potential instability can then lead to vigorous convection. Potential instability is defined in terms of the wet-bulb potential temperature θ_w (Section 3.5.7). A given value of θ_w can unambiguously be attributed to an individual saturated adiabat. The higher the specific humidity of an air parcel at a given temperature, the sooner the parcel will reach its LCL upon lifting and therefore the higher θ_w is. The vertical profile of θ_w is thus a measure of the vertical distribution of moisture in the layer.

The examples shown in Figure 4.4 are chosen in such a way that the layer between 1000 and 900 hPa is dry unstable in all three cases, in which θ decreases from 1000 to 900 hPa, corresponding to the right example in Figure 4.3. The situation is potentially stable on the left ascent, with θ_w increasing with altitude from $\theta_w^{base} = 3\,°\text{C}$ at 1000 hPa to $\theta_w^{top} = 7\,°\text{C}$ at 900 hPa. In this example, the water vapor mixing ratio is higher at the top than at the bottom of the layer, so the LCL is reached immediately at the top of the layer but only after some dry adiabatic ascent at the bottom of the layer. Condensation occurs at 900 hPa throughout the layer. As the top of the layer experiences more latent heat release during lifting, it does not cool

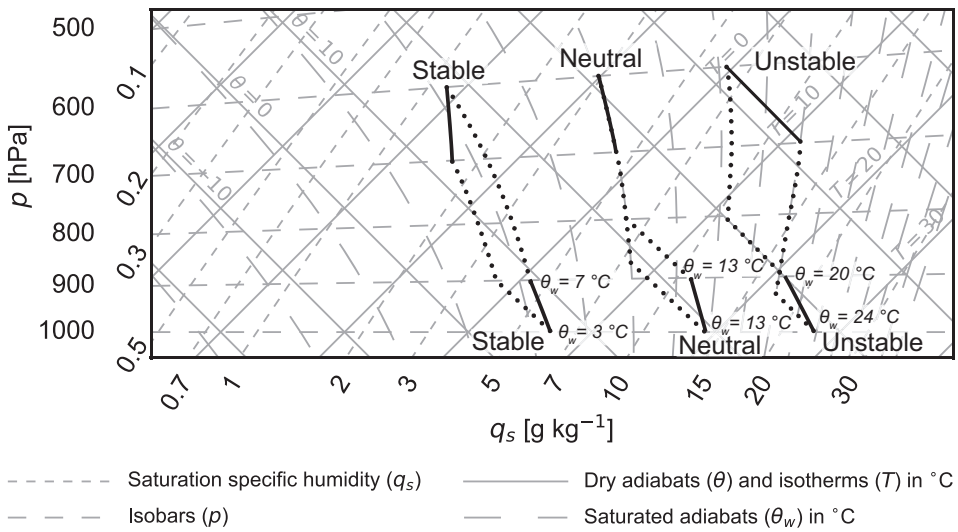


Figure 4.4 Schematic of the lifting of a layer of moist air from 1000–900 hPa to 700–600 hPa for three cases, where the layer is potentially stable, potentially neutral, or potentially unstable. The bold solid lines represent the lapse rate in the layer before and after lifting. The dotted lines show the ascent of the top and the bottom of the layer.

https://doi.org/10.1017/9781009485654.005 Published online by Cambridge University Press

Table 4.5 Static stability criteria for the lifting of layers of moist air.

$\partial\theta_w/\partial z > 0$	Potentially stable layer
$\partial\theta_w/\partial z = 0$	Potentially neutral layer
$\partial\theta_w/\partial z < 0$	Potentially unstable layer

as much as the bottom of the layer, so that the dry stability after lifting has been reversed. It is now a dry stable situation with θ increasing from $\theta^{base} = 12\,^{\circ}\mathrm{C}$ at 700 hPa to $\theta^{top} = 17.5\,^{\circ}\mathrm{C}$ at 600 hPa. Note that θ_w is conserved during layer lifting.

In the potentially neutral case (middle ascent in Figure 4.4), the vertical moisture distribution is such that condensation is reached at 900 hPa at the base of the layer and at 840 hPa at the layer top. Here, $\theta_w = 13\,^{\circ}\mathrm{C}$ is constant throughout the 1000–900 hPa layer and does not change upon lifting.

In the potentially unstable case (right ascent in Figure 4.4), θ_w decreases with increasing altitude. In this example, the situation is chosen such that the layer is very dry at the top and very moist at the bottom, which represents a layer of air just underneath an inversion at the top of the PBL. In this case, the top of the layer cools dry adiabatically until approximately 790 hPa, which corresponds to $\theta_w^{top} = 20\,^{\circ}\mathrm{C}$, whereas the base reaches its LCL already at 960 hPa, which corresponds to $\theta_w^{base} = 24\,^{\circ}\mathrm{C}$. These criteria for potential instability are summarized in Table 4.5.

4.6 Horizontal Air Motions

In this section, we consider the horizontal displacement of air, initiated by the pressure gradient force. In the free troposphere, the air motion is not affected by friction. In the PBL, friction changes both the direction and the speed of the wind, as we will see in Section 4.6.4.

4.6.1 Gradient Wind

The most general wind balance in the absence of friction is called the *gradient wind balance*. It results from a balance between the pressure gradient force $\partial p/\partial r$, the Coriolis force fv_t, and the centrifugal force v_t^2/r. A good example of the gradient wind balance is the horizontal wind circulation around a tropical cyclone in the free troposphere (Chapter 11). Because the isobars in a gradient wind balance are curved, the gradient wind is best described in cylindrical coordinates, where r is pointing outwards and v_t is the tangential component of the gradient wind around the pressure minimum. The gradient wind balance is given as

$$\underbrace{\frac{1}{\rho_a}\frac{\partial p}{\partial r}}_{\text{pressure gradient force}} = \underbrace{\frac{v_t^2}{r}}_{\text{centrifugal force}} + \underbrace{fv_t}_{\text{Coriolis force}} . \tag{4.48}$$

https://doi.org/10.1017/9781009485654.005 Published online by Cambridge University Press

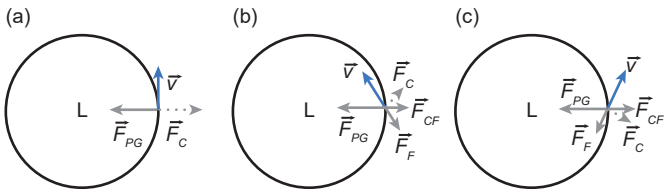


Figure 4.5 Schematic of different wind balances in the northern hemisphere: (a) gradient wind, (b) subgradient wind, (c) supergradient wind. L denotes the low-pressure center.

The gradient wind balance is schematically shown in Figure 4.5a. The gradient wind balance can be simplified for two extremes: (i) when the centrifugal force is negligible, it can be approximated with the *geostrophic wind balance* (Section 4.6.2) and (ii) when the Coriolis force is negligible, it can be approximated with the *cyclostrophic wind balance* (Section 4.6.3).

Which type of simplification is appropriate can be determined from the dimensionless *Rossby*[8] *number Ro*. *Ro* is the ratio of the inertial force, that is, horizontal advection term, to the Coriolis force in the Navier–Stokes equation (eq. 4.1) for a flow of a rotating fluid. A scale estimate of the advection term from Table 4.1 yields: U^2/L. Taking fU as the scale estimate for the Coriolis force leads to the definition of *Ro*:

$$Ro = \frac{U^2}{LfU} \text{ or } \frac{U}{fL}. \tag{4.49}$$

4.6.2 Geostrophic Wind

The geostropic wind describes the balance between the pressure gradient force and the Coriolis force. The flow can be assumed to be in geostrophic wind balance when the curvature of the isobars in the free troposphere is small. Mathematically speaking, the geostrophic flow is applicable for $Ro < 1$, that is, at large scales where the Coriolis force dominates over the inertial force. With the values in Table 4.1, we obtain for midlatitude synoptic systems: $Ro = \frac{U}{fL} = \frac{10\,\mathrm{m\,s^{-1}}}{10^{-4}\,\mathrm{s^{-1}} \cdot 10^{6}\,\mathrm{m}} = 0.1$.

Consequently, the large-scale horizontal atmospheric motion is often approximated by a steady-state geostrophic flow, in which the Coriolis force almost exactly balances the horizontal pressure gradient force. In steady-state, the acceleration is zero, hence this wind is constant in time. The geostrophic wind can be obtained from a scale analysis of the horizontal components of the Navier–Stokes equation (eq. 4.1), here, for example, for the zonal wind component u (eq. 4.8) at 45 °N.

Neglecting friction outside the PBL and using typical synoptic scale values as given in Table 4.1, the following orders of magnitude can be obtained for the individual terms in eq. (4.8):

[8] www.britannica.com/biography/Carl-Gustaf-Arvid-Rossby

https://doi.org/10.1017/9781009485654.005 Published online by Cambridge University Press

$$F_{PG,x} \approx \frac{\Delta p}{\rho_a L} = 10^{-3}\,\mathrm{m\,s^{-2}}, \tag{4.50}$$

$$F_{C,x_v} \approx fU = 10^{-3}\,\mathrm{m\,s^{-2}}, \tag{4.51}$$

$$F_{C,x_w} \approx fW = 10^{-6}\,\mathrm{m\,s^{-2}}, \tag{4.52}$$

$$\frac{\partial u}{\partial t} \approx \frac{U}{t_{hor}} = 10^{-4}\,\mathrm{m\,s^{-2}}, \tag{4.53}$$

$$u\frac{\partial u}{\partial x} \approx \frac{U^2}{L} = 10^{-4}\,\mathrm{m\,s^{-2}}. \tag{4.54}$$

We start by acknowledging that the large-scale vertical air motion W is three orders of magnitude smaller than the horizontal air motion U. Hence, the contribution of the vertical air motion to the x-component of the Coriolis force $F_{C,x_w} \approx 10^{-6}\,\mathrm{m\,s^{-2}}$ in eq. (4.8) can be neglected and F_{C,x_v} can be approximated with $F_{C,x}$. The inertial term and the time derivative, are both about an order of magnitude smaller than $F_{C,x}$ and $F_{PG,x}$ and thus can also be neglected. We then arrive at the simplified equation for the x-component of the Navier–Stokes equation:

$$fu_g = -\frac{1}{\rho_a}\frac{\partial p}{\partial y}. \tag{4.55}$$

Similarly, the y-component of the Navier–Stokes equation can be simplified with these approximations to:

$$fv_g = \frac{1}{\rho_a}\frac{\partial p}{\partial x}. \tag{4.56}$$

These equations thus define the geostrophic wind:

$$\vec{v}_g = \frac{1}{f\rho_a}\vec{k} \times \vec{\nabla}_h p, \qquad u_g = -\frac{1}{f\rho_a}\frac{\partial p}{\partial y}, \qquad v_g = \frac{1}{f\rho_a}\frac{\partial p}{\partial x}. \tag{4.57}$$

The geostrophic wind describes the exact balance between the Coriolis force and the horizontal pressure gradient force, in which the (geostrophic) wind blows parallel to the isobars. Such a steady-state flow with equal forces is only possible in the absence of friction, that is, above the PBL.

The geostrophic wind balance strinctly speaking requires parallel straight isobars, but in practice is considered when the Coriolis force dominates over the inertial force. In the example shown in Figure 4.6, an air parcel is initially at rest at point A and hence does not experience any Coriolis force. In a pressure field, the air parcel starts to move down the horizontal pressure gradient from the high-pressure region to the low-pressure region (see point B in Figure 4.6). With increasing wind speed, the Coriolis force increases and the parcel is deflected (to the right-hand side in the direction of motion on the northern hemisphere; Section 4.1). Once the parcel's trajectory is deflected so far that the direction of the Coriolis force is of opposite sign but equal in magnitude to the pressure gradient force (i.e., the lengths of solid and dotted arrows depicted in Figure 4.6 become equal), the parcel moves perpendicular to

https://doi.org/10.1017/9781009485654.005 Published online by Cambridge University Press

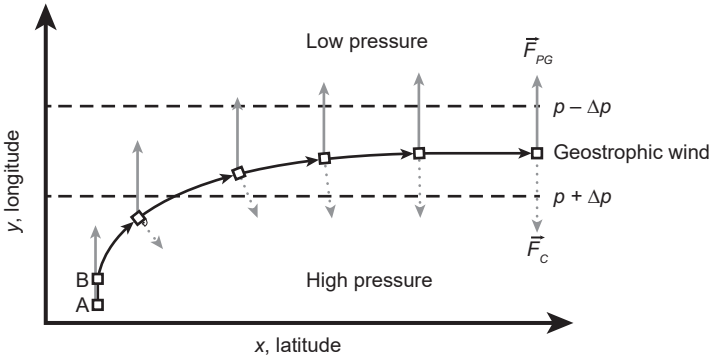


Figure 4.6 Schematic of an air parcel (small squares) approaching geostrophic wind balance in the northern hemisphere: An air parcel initially at rest at point A starts to move along the negative pressure gradient until $\vec{F}_{PG}$ (solid gray arrows) and $\vec{F}_C$ (dotted gray arrows) are of equal magnitude but opposite sign. The broken lines denote isobars.

the pressure gradient (eq. 4.57) and the wind blows parallel to the isobars. Over the northern hemisphere, the low-pressure system is on the left side in the direction of the geostrophic flow and the high pressure is on the right side (and vice versa on the southern hemisphere). Because the Coriolis parameter f is zero at the equator, the geostrophic wind is not defined at the equator.

The above geostrophic balance results from the speed at which Earth rotates. If Earth were to rotate much more slowly, friction rather than the Coriolis force would limit the wind speed. If Earth rotated faster, the geostrophic balance would qualitatively be the same, but because f would be larger, the balance would be achieved at smaller velocities.

4.6.3 Cyclostrophic Wind

The gradient wind balance can also be simplified when the horizontal extent of the vortex is so small that the inertial force dominates over the Coriolis force. This is the case for small-scale circulations, for example, for circulations around a tornado in midlatitudes, for which the Rossby number is given as: $Ro = \frac{U}{fL} = \frac{10^2\,\mathrm{m\,s^{-1}}}{10^{-4}\,\mathrm{s^{-1}} \cdot 10^2\,\mathrm{m}} = 10^4$. Hence, the Coriolis force can be neglected.

The wind that results from the force balance between the pressure gradient force and the centrifugal force is called the cyclostrophic wind and is given as:

$$\frac{1}{\rho_a}\frac{\partial p}{\partial r} = \frac{v_t^2}{r}. \tag{4.58}$$

https://doi.org/10.1017/9781009485654.005 Published online by Cambridge University Press

4.6.4 Horizontal Wind with Friction

In the atmosphere, the geostrophic approximation is often used to describe the movement of horizontal air masses outside the PBL, where the assumption of a friction-less flow is reasonable. In the PBL, however, a frictional drag is exerted on the air by the surface, slowing down the air motion. This leads to the logarithmically increasing horizontal wind speed with increasing altitude in the PBL (Stull, 1988), as illustrated in Figure 4.7.

The slowing down of the wind near the surface due to friction reduces the Coriolis force, making a balance between the Coriolis force and the pressure gradient force impossible. In this case, the wind speed results from considering the Coriolis force, the pressure gradient force, and an ageostrophic component, due to friction. The ageostrophic flow is thus the difference between the (idealized) geostrophic flow and the actual flow. Contrary to the geostrophic flow, the ageostrophic flow does not blow parallel to the isobars, but from the high to the low pressure, thus allowing for mass transport toward the centers of low-pressure systems.

Most atmospheric flows, especially the inflows in midlatitude low-pressure systems and tropical cyclones, deviate from the gradient wind (eq. 4.48) and have a pronounced ageostrophic component.

If the ageostrophic component is directed toward the center of the low pressure, the resulting wind is called the *subgradient wind*. Subgradient wind arises due to the decrease in the tangential wind speed caused by friction such that the pressure-gradient force is larger than the sum of the centrifugal and Coriolis forces (Figure 4.5b):

$$\frac{1}{\rho_a}\frac{\partial p}{\partial r} > \frac{v_t^2}{r} + f v_t. \tag{4.59}$$

The opposite case, in which the pressure-gradient force is smaller than the sum of the centrifugal and Coriolis forces, is called *supergradient wind* (Figure 4.5c) and is directed away from the low-pressure center:

$$\frac{1}{\rho_a}\frac{\partial p}{\partial r} < \frac{v_t^2}{r} + f v_t. \tag{4.60}$$

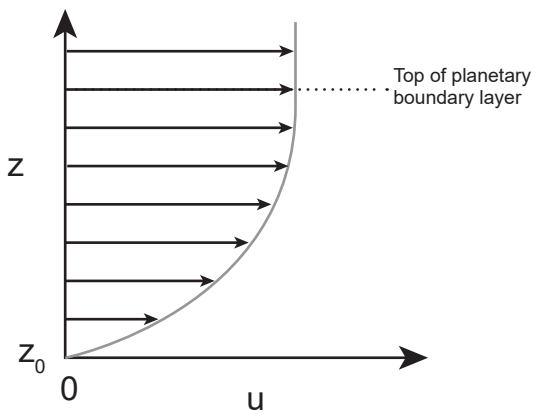


Figure 4.7 Schematic of the logarithmic wind profile: change in the horizontal wind with altitude in the planetary boundary layer.

https://doi.org/10.1017/9781009485654.005 Published online by Cambridge University Press

4.6.5 Thermal Wind

In a barotropic atmosphere, where the density is only a function of pressure, but independent of temperature, the horizontal pressure gradient and the geostrophic wind are constant with altitude. In the real atmosphere, the density depends on both pressure and temperature, as evident from the ideal gas law (eq. 3.7). In such an atmosphere, the larger the distance between two pressure levels, the higher the (virtual) temperature of its air, according to the hypsometric equation (eq. 4.15). In the latter case, termed a *baroclinic atmosphere*, the horizontal pressure gradient varies with altitude. This in turn implies that the geostrophic wind also varies with altitude. The cause for this variation is the non-uniform temperature distribution in the horizontal or, put differently, that the isotherms are not parallel to the isobars, as depicted in Figure 4.8. The variation in the geostrophic wind with altitude in a baroclinic atmosphere is called the geostrophic wind shear or the *thermal wind*. One example of the thermal wind is the *jet streams*, which result from the increase in wind speed with height. The thermal wind has its origin in the horizontal temperature gradient on isobaric surfaces, denoted by subscript p in the following equations, and is directed parallel to the isotherms. The thermal wind components are given as (Holton and Hakim, 2012):

$$\begin{aligned} p\frac{\partial u_g}{\partial p} &= \frac{R_d}{f}\left(\frac{\partial T}{\partial y}\right)_p, \\ p\frac{\partial v_g}{\partial p} &= -\frac{R_d}{f}\left(\frac{\partial T}{\partial x}\right)_p. \end{aligned} \tag{4.61}$$

These equations show that the horizontal temperature gradient causes a vertical geostrophic wind shear. Applying the hydrostatic equation (eq. 4.47) to replace partial derivatives with respect to pressure p with those with respect to altitude z, and making use of the ideal gas law (eq. 3.94), yields

$$\begin{aligned} f\frac{\partial u_g}{\partial z} &= -\frac{g}{T}\left(\frac{\partial T}{\partial y}\right)_p, \\ f\frac{\partial v_g}{\partial z} &= \frac{g}{T}\left(\frac{\partial T}{\partial x}\right)_p. \end{aligned} \tag{4.62}$$

Because the partial derivatives of temperature with respect to x and y are to be taken at constant pressure, T can be replaced with θ so that the thermal wind equations become:

$$\begin{aligned} f\frac{\partial u_g}{\partial z} &= -\frac{g}{\theta}\left(\frac{\partial \theta}{\partial y}\right)_p, \\ f\frac{\partial v_g}{\partial z} &= \frac{g}{\theta}\left(\frac{\partial \theta}{\partial x}\right)_p. \end{aligned} \tag{4.63}$$

That is, if θ is not uniform in the horizontal direction, the geostrophic wind will change with altitude and initiate a thermal wind. A typical situation of the thermal wind in midlatitudes in the northern hemisphere is shown in Figure 4.8. The depicted example can be thought of as the subtropics, characterized by high-pressure systems, for example, the Azores high with warm air masses, and midlatitudes characterized by low-pressure systems, for example, the Aleutian and Icelandic lows with cold air masses. Between them exists horizontal temperature

https://doi.org/10.1017/9781009485654.005 Published online by Cambridge University Press

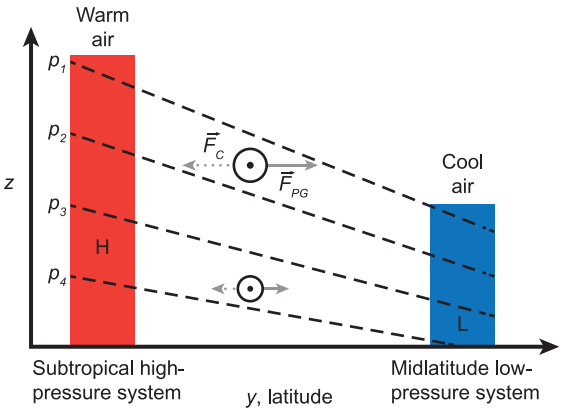


Figure 4.8 Schematic of the thermal wind for a typical location in the midlatitudes of the northern hemisphere. In this example, the wind blows in the direction perpendicular to the page, toward the observer. Isobars are shown as broken lines, with pressure decreasing from p_4 to p_1. The solid gray arrows indicate the pressure gradient force $\vec{F}_{PG}$ and the dotted gray arrows show the Coriolis force $\vec{F}_C$. The red region denotes warm air as found in the subtropics and high pressure (H) and the blue region cool air and low pressure (L) as found in midlatitude low-pressure systems.

and pressure gradients. Because of the hypsometric equation (eq. 4.15), the vertical distance between two isobars is larger in the warm subtropical air than in the cold polar air. Thus, the horizontal pressure gradient increases with increasing altitude, increasing the horizontal wind speed and hence the Coriolis force. As a consequence, the geostrophic wind increases with increasing altitude, which explains the high wind speeds of the polar and subtropical jet streams.

4.6.6 Inertial Instability

While knowledge of the vertical distribution of the potential temperature allows us to characterize the static stability of the atmosphere, knowledge of the horizontal distribution of the *absolute momentum* M, also called absolute linear momentum, allows us to characterize the *inertial stability*, that is, the horizontal stability of the atmosphere (Holton and Hakim, 2012). For a flow in the x-direction, M is defined as the momentum due to Earth's rotation, fy, minus the geostrophic wind, u_g, also referred to as the linear momentum:

$$M = fy - u_g. \tag{4.64}$$

In the absence of friction, M is conserved, that is, $dM/dt = 0$. The conservation of M for horizontal displacements is the analog of the conservation of θ ($d\theta/dt = 0$) for vertical displacements in dry adiabatic conditions (eq. 3.30). The expression for M in the y-direction can

https://doi.org/10.1017/9781009485654.005 Published online by Cambridge University Press

be derived from the x-component of the Navier–Stokes equation (4.8), assuming a constant Coriolis parameter f and neglecting friction:

$$\frac{du}{dt} = -\frac{1}{\rho_a}\frac{\partial p}{\partial x} + fv. \tag{4.65}$$

Let us consider an initial geostrophic flow in the x-direction (Figure 4.9). At the location x_0, the pressure gradient $\partial p/\partial x$ is zero, so that

$$\frac{du_g}{dt} - fv = \frac{d}{dt}(u_g - fy) = -\frac{dM}{dt} = 0. \tag{4.66}$$

Suppose that at y_0, the parcel is suddenly displaced in the positive y-direction without perturbing the pressure field (Figure 4.9). Then the y-component of the Navier–Stokes equation is given as

$$\frac{dv}{dt} = -\frac{1}{\rho_a}\frac{\partial p}{\partial y} - fu = f(u_g - u), \tag{4.67}$$

where we have made use of the definition of the geostrophic wind (eq. 4.57). This equation states that the air parcel experiences an acceleration in the y-direction if the geostrophic wind u_g exceeds the actual zonal wind u.

For the situation depicted in Figure 4.9, $\partial p/\partial y$ is negative and thus u_g is positive. The acceleration of the air parcel toward the low-pressure region increases the Coriolis force until it reaches its maximum at point x_2 in Figure 4.9. Here, the Coriolis force component in the x-direction is zero but the component in the negative y-direction is non-zero, causing the air parcel to move toward the high-pressure region and therefore to experience a deceleration. Because the Coriolis force lags behind the acceleration caused by the pressure gradient force,

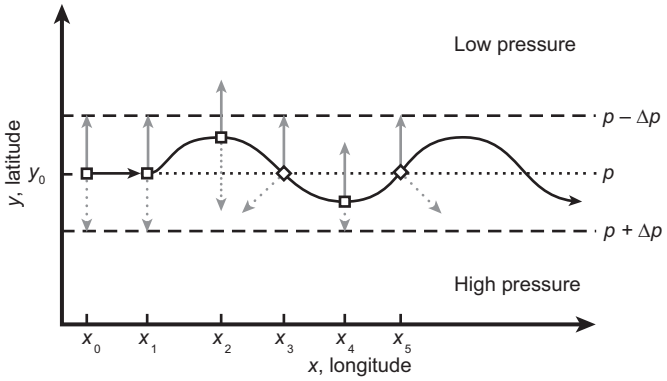


Figure 4.9 Schematic of an inertial oscillation (solid curve) of an air parcel (black squares) in an x–y plane. The solid gray arrows indicate the pressure gradient force $\vec{F}_{PG}$ and the dotted gray arrows indicate the Coriolis force $\vec{F}_C$. The dotted and dashed black lines denote isobars. The initial position, from which the air parcel in a geostrophic flow is displaced, is denoted by y_0.

https://doi.org/10.1017/9781009485654.005 Published online by Cambridge University Press

the result is an oscillatory motion. An atmospheric example for such an inertial wave are extratropical Rossby waves (Rossby, 1940) that form in mid latitudes when warm tropical air moves toward the poles and cold polar air moves equatorwards.

The horizontal shear of M equals the *absolute vorticity*. The vertical component of the absolute vorticity is the sum of the *relative vorticity* $\zeta = \partial v/\partial x - \partial u/\partial y$ and the *planetary vorticity* from the Earth, which equals the Coriolis parameter f. In a two-dimensional geostrophic flow in the x-direction where $\partial v/\partial x = 0$, we obtain the horizontal shear of M by taking the derivative with respect to y:

$$\frac{\partial M}{\partial y} = \underbrace{f - \frac{\partial u_g}{\partial y}}_{\text{abs. vorticity}}. \tag{4.68}$$

While the Brunt–Väisälä frequency determines the frequency of oscillation in a statically stable atmosphere, in an inertially stable atmosphere, the frequency of oscillation is the product of the Coriolis parameter and the horizontal shear of the absolute momentum, which we will derive now. To obtain the analogous equation to that for a static oscillation (eq. 4.34), we assume that the air parcel is displaced from y_0 (Figure 4.9) by $\tilde{y}$ in the positive y-direction, where the new zonal geostrophic wind can be approximated using a truncated Taylor series:

$$u_g(y_0 + \tilde{y}) = u_g(y_0) + \left.\frac{\partial u_g}{\partial y}\right|_{y=y_0} (y - y_0). \tag{4.69}$$

Likewise, for the new zonal wind, we have

$$u(y_0 + \tilde{y}) = u(y_0) + \left.\frac{\partial u}{\partial y}\right|_{y=y_0} (y - y_0). \tag{4.70}$$

Now assume that the zonal wind equals the zonal geostrophic wind at y_0, that is, $u(y_0) = u_g(y_0)$. At this point, the zonal wind does not experience a pressure gradient force in the x-direction and we can obtain the change in u with y from eq. (4.65):

$$\frac{du}{dt} = fv = f\frac{dy}{dt}. \tag{4.71}$$

Upon time integration and taking the derivative with respect to y, we obtain $\partial u/\partial y = f$. Inserting this together with $u(y_0) = u_g(y_0)$ into eq. (4.70) yields

$$u(y_0 + \tilde{y}) = u_g(y_0) + f(y - y_0). \tag{4.72}$$

Inserting eqs. (4.69) and (4.72) into eq. (4.67), associating v with $d\tilde{y}/dt$, and noting that $y - y_0 = \tilde{y}$ yields the equation for the inertial oscillation:

$$\frac{d^2\tilde{y}}{dt^2} + f\left(f - \frac{\partial u_g}{\partial y}\right)\tilde{y} = \frac{d^2\tilde{y}}{dt^2} + f\frac{\partial M}{\partial y}\tilde{y} = 0. \tag{4.73}$$

The solution is of the form $\tilde{y}(t) = A\exp(\pm i\sqrt{f(\partial M/\partial y)}t)$. If M decreases with increasing y in the northern hemisphere, where $f > 0$, then the absolute vorticity is negative and the situation is inertially unstable. If M increases with increasing y, we obtain stable sinusoidal oscillations (undamped harmonic oscillations). This means that an air parcel accelerated in the positive

https://doi.org/10.1017/9781009485654.005 Published online by Cambridge University Press

Table 4.6 Criteria for inertial stability for a two-dimensional geostrophic flow in the $x-y$ plane, where the oscillation is along the x-direction.

$\partial M/\partial y > 0$	Inertially stable
$\partial M/\partial y = 0$	Inertially neutral
$\partial M/\partial y < 0$	Inertially unstable

y-direction toward the lower pressure will experience a larger Coriolis force due to its higher velocity, and it will be pulled back toward the higher pressure in the negative y-direction. If the air parcel has too much momentum and overshoots toward the higher pressure, it will experience a negative acceleration and will again move toward the lower pressure. The stability criteria are summarized in Table 4.6.

Inertial instability occurs most frequently in the tropics (Thompson et al., 2018) and decreases polewards. The flow in extratropical synoptic-scale systems is mostly inertially stable (Holton and Hakim, 2012). However, inertial instability on the synoptic scale does occur within ridges and anticyclonic-shear zones of the polar jet (Thompson et al., 2018).

4.7 Slantwise Displacement

Static instability matters for purely vertical displacement caused by buoyancy. Inertial instability matters for purely horizontal displacement caused by an imbalance between the Coriolis, cyclostrophic and pressure gradient forces. Yet, symmetric instability can occur if the atmosphere is stable for pure horizontal displacement and pure vertical displacement, but unstable to slantwise displacement. Slantwise displacement refers to the diagonal movement of an air parcel in the atmosphere, combining both horizontal and vertical motion. The associated stability or instability is thus referred to as *slantwise stability* or *slantwise instability*. One prominent example of slantwise instability is *symmetric instability* (Schultz and Schumacher, 1999). It is thought to accelerate the upper tropospheric outflow from TCs (Molinari and Vollaro, 2014) and to cause frontal rainbands in extratropical cyclones (Bennetts and Hoskins, 1979; Clark and Gray, 2018; Zhao et al., 2022, Chapter 10) or in squall lines (Colby et al., 2022, Chapter 11).

In a statically and inertially stable atmosphere, slantwise displacement leading to slantwise instability of an air parcel can occur if the mean horizontal wind exhibits vertical shear. This is the case in Figure 4.10, as explained next. According to eq. (4.64), a decrease of M with increasing altitude at any given latitude y implies that u_g increases with increasing altitude. In situations where buoyancy is the vertical force in a slantwise displacement process, slantwise displacement occurs in the form of slantwise convection. In addition to the vertical buoyancy

https://doi.org/10.1017/9781009485654.005 Published online by Cambridge University Press

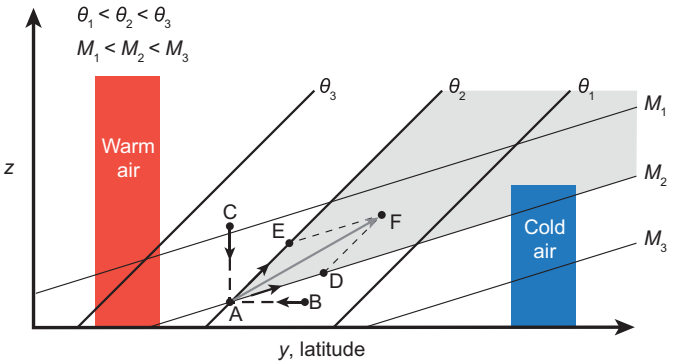


Figure 4.10 Schematic of a vertical cross-section in the northern hemisphere. Symmetric instability arises in the gray-shaded region exemplified for an air parcel that is deflected from an equilibrium condition at point A to point F. Isolines are shown of absolute momentum M, increasing from M_1 to M_3, and of potential temperature θ, increasing from θ_1 to θ_3. A purely horizontal (A to B) or purely vertical (A to C) displacement would result in a counteracting movement back to point A because of inertial or static stability, respectively, (dashed lines with the backward pointing arrows).

force, a horizontal force that will initiate a horizontal motion (i.e., Coriolis, pressure gradient and/or centrifugal force) is needed for slantwise convection to occur.

Let us assume an atmosphere with a horizontal temperature gradient in which the isentropic surfaces (constant-θ surfaces) are tilted as illustrated in Figure 4.10. As shown in Figure 4.11b, this is the common situation in the troposphere. Such tilted isentropes arise because of a horizontal temperature gradient, indicated by the warm and cold air in Figure 4.10. Pure vertical isentropes, on the other hand, would indicate a statically dry neutral atmosphere.

In the absence of a horizontal temperature gradient in the y-direction, that is, in a barotropic atmosphere, the θ surfaces are oriented horizontally. In such an atmosphere, a horizontal displacement in the y-direction of an air parcel would be neutral because θ remains constant during the displacement. In a barotropic atmosphere, the M-surfaces are oriented vertically. Such an atmosphere is neutral both to static and to inertial instability.

Now consider a baroclinic atmosphere, and suppose that an air parcel at point A in Figure 4.10 is in equilibrium with the environment (i.e., it has the same T, p, u, v). Next, suppose that the air parcel is slantwise displaced to point F, that is, the air parcel is displaced both horizontally and vertically. By buoyancy alone, the air parcel would rise vertically from point A to point C. In Figure 4.10, θ increases from A to C, such that the atmosphere is statically stable and the air parcel will experience a counteracting force back to point A. Likewise, an air parcel that is pushed from A to B will experience a counteracting movement back to point A, as M is increasing from A to B in this inertially stable environment.

For the air parcel to be slantwise displaced from A to F, an imbalance between the horizontal pressure gradient and the inertial forces is required, such that the air parcel is also

https://doi.org/10.1017/9781009485654.005 Published online by Cambridge University Press

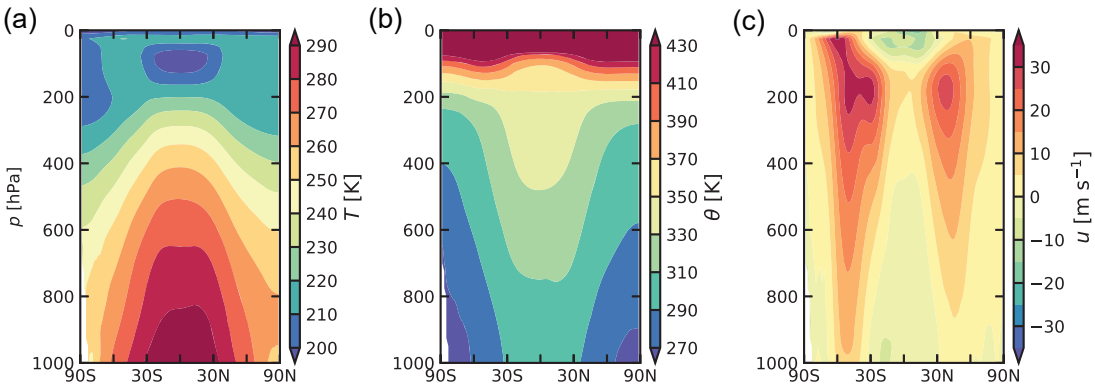


Figure 4.11 Annual and zonal mean latitude versus pressure distribution of (a) temperature, (b) potential temperature, and (c) the zonal wind, based on 10-year (2003–2012) climatology simulated with the ECHAM6-HAM2 climate model (Neubauer et al., 2019).

displaced in the meridional direction, that is, in the positive y-direction for the example in Figure 4.10. In addition to the potential temperature θ gradient, we need to consider the gradient of the absolute momentum surfaces M, since this determines whether a horizontal displacement will be further displaced or will experience a restoring force. For a baroclinic flow, in which the mean westerly flow increases with height (Figures 4.8 and 4.11c), both the θ and M-surfaces slope upward toward the pole, as shown schematically in Figure 4.10. Also, in the annual zonal mean, the atmospheric θ values slope upward toward the poles, as shown in Figure 4.11b.

If the buoyancy force is zero, that is, if the parcel displacement occurs along an isentropic surface, for example, along the θ_2 isentrope from points A to E in Figure 4.10, then the parcel has a lower absolute momentum at point E (between M_1 and M_2) then where it started at A (M_2). In other words, the path A $\rightarrow$ E is inertially unstable, but statically neutral. Likewise, if the parcel displacement occurs along a M-surface, for example, from A to D, then the parcel has a lower θ in D (between θ_1 and θ_2) then where it started at A (θ_2). Hence, the path A $\rightarrow$ D is statically unstable, but inertially neutral.

The condition for symmetric instability in an atmosphere that is internally and statically stable is that M decreases with increasing y on a θ-surface (isentropes) and/or that θ decreases with increasing z on an M-surface (Table 4.7). In Figure 4.10, this is the case for an air parcel being deflected from A to D, E or F. Conditions for symmetric instability prevail in the atmosphere when the M-surfaces are tilted more from the vertical than the θ-surfaces, as depicted in Figure 4.10. The typical situation in the atmosphere is the opposite, in which the M-surfaces are tilted less from the vertical than the isentropes. Thus, the atmosphere is generally symmetrically stable.

More generally speaking, symmetric instability is often used as being synonymous to inertial instability. This is because inertial instability acts on longer timescales than static instability. The latter is quickly removed by convection. Therefore, regions of symmetric instability can coincide with regions of inertial instability, given that the absolute momentum M decreases with increasing latitude y occur along a constant θ-surface.

https://doi.org/10.1017/9781009485654.005 Published online by Cambridge University Press

Table 4.7 Criteria for symmetric stability.

$\partial\theta/\partial z\|_M > 0$ or $\partial M/\partial y\|_\theta > 0$	Symmetrically stable atmosphere
$\partial\theta/\partial z\|_M = 0$ or $\partial M/\partial y\|_\theta = 0$	Symmetrically neutral atmosphere
$\partial\theta/\partial z\|_M < 0$ and/or $\partial M/\partial y\|_\theta < 0$	Symmetrically unstable atmosphere

An example for the first criterion for symmetric instability $\partial\theta/\partial z\,|_M < 0$ in Table 4.7 would be free convection along a constant M-surface, that is, the decrease of θ with altitude is caused by the air moving along a M-surface. In the case where symmetric instability coincides with inertial instability, the latter criterion $\partial M/\partial y\,|_\theta < 0$ is fulfilled. This is often the case in the ouflow regions of a tropical cyclone (Molinari and Vollaro, 2014).

https://doi.org/10.1017/9781009485654.005 Published online by Cambridge University Press